Chalcogenide Letters Vol. 8, No. 4, April 2011, p. 231 – 237

EFFECT OF THICKNESS ON THE STRUCTURAL AND OPTICAL PROPERTIES OF ZnS THIN FILMS PREPARED BY FLASH EVAPORATION TECHNIQUE EQUIPPED WITH MODIFIED FEEDER

H. REZAGHOLIPOUR DIZAJI*, A. JAMSHIDI ZAVARAKI, M. H. EHSANI
Thin Film Lab., Physics Department, Semnan University, Semnan 35195-363, I. R. Iran

ZnS thin layers have been deposited on glass substrate by flash evaporation technique equipped with a modified feeder. This new feeder is an additional system to flash evaporation technique which gives a better control to materials transferring into boat in thermal evaporation coating system. In the present work, using this method, ZnS thin films of 100nm, 300nm and 500nm thick were made successfully for structural and optical properties studies. The specimens were characterized using x-ray diffraction and UV-Vis spectrophotometer. The structural characterization revealed a cubic phase for all of the grown ZnS films. From analyzed optical data, it was found that the optical parameters, namely, absorbance, transmittance, band gap energy and refractive index changed upon increasing the thickness of samples.

(Received March 15, 2011; Accepted April 7, 2011)

Keywords: Flash evaporation: Thin films; Zinc sulfide; Structural properties; Optical properties

1. Introduction

ZnS and other chalcogenide compounds are interesting optoelectronic materials [1].

Zinc sulfide belongs to the II–VI family of semiconducting materials receiving ever increasing attention due to its wide variety of applications such as UV-light-emitting diodes [2] and efficient phosphors in flat-panel displays [3, 4]. It has potential applications in mesoscopic electronic and optical devices [5]. It can crystallize in two allotropic forms: a cubic form (c-ZnS) with sphalerite structure and a hexagonal form (h-ZnS) with wurtzite structure. The normal phase transition temperature is 1020 °C, but both the structures can be present at ambient temperature [6]. Many important properties of interest for such applications are determined by the ZnS thin film microstructure developed during the deposition process. For instance, the electro-luminescence characteristics such as threshold voltage, saturation brightness, steepness of the curve B-V (brightness-voltage), and the device lifetime depend primarily on grains size [7]. ZnS thin films have been prepared by various techniques such as sputtering [8], chemical vapor deposition (CVD) [9], spray paralysis [10], photochemical deposition [11], Electrochemical deposition [12], pulsed laser deposition [13] and thermal evaporation [14 and 15]. Compared to some sophisticated techniques, vacuum thermal evaporation is very simple and inexpensive which can be used for large area thin film deposition. The problem associated with this technique is maintaining the stoichiometry in the deposition of materials composed of different melting points such as ZnS. Hence flash evaporation technique (FET) has been used by many researchers to overcome the said problem [16-22].

*Corresponding author: hrdizajii@gmail.com

The main idea in FET is to transfer the starting material into the boat heated up to the melting point element available in it, so as to evaporate the material once it falls inside the boat.

In this report, the authors have employed their new design of feeder in FET for the fabrication of ZnS thin films [23]. The samples have been prepared successfully in different thicknesses to investigate their structural and optical properties. The mentioned properties of the films have been studied by XRD and UV-Vis spectrophotometer.

2. Experimental

ZnS films of 100, 300 and 500 nm thick were deposited on glass substrates using FET equipped with new feeder in a HINDIHIVAC coating unit (Model15F6). The substrates were cleaned in acetone and methanol using ultrasonic bath and then dried by nitrogen gas. Further, the substrates were subjected to glow discharge cleaning before deposition.

ZnS powder of 99.99% purity supplied by Aldrich Company was placed in some bins of rotating disk (Fig.1). When the vacuum chamber reached to the 10^{-6} mbar pressure, the revolving disk was rotated by a mechanical feedthrough. In appropriate place, just above the cone, the shutter of bin was removed by a mechanical barrier so that the material could be transferred into the ablazing molybdenum boat. The material was immediately vaporized. The deposition rate was measured in situ by using HindHiVac thickness monitor (Model DTM-101). The typical growth rate was about 2.5Å/s. The source-to-substrate distance was approximately 15cm. All the films were deposited on substrate maintained at ambient temperature in vacuum chamber. After deposition, the films were removed from the coating chamber and exposed to the ambient atmosphere. X-ray diffraction (XRD) was employed to investigate the crystal structure of ZnS films. This study was carried out on an x-ray diffractometer (ADVANCE MODEL D8) with high intensity Cuk_{α} radiation (λ=1.5406 Å).The optical absorbance as well as transmittance spectra of ZnS thin films were obtained in UV-Vis spectrophotometer (shimatsu Model UV-1650 PC).

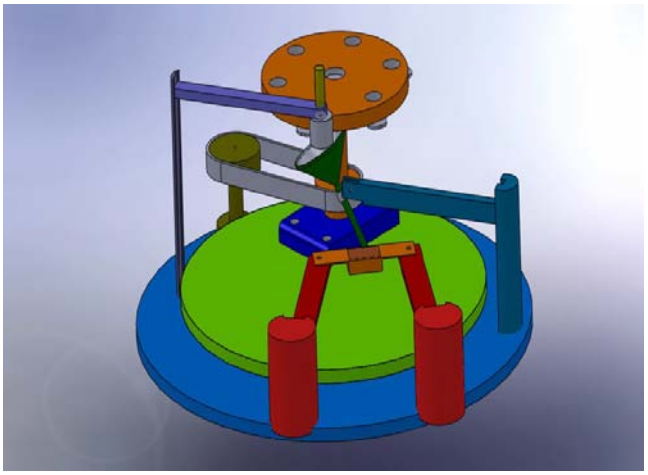

Fig.1: The FET joined with designed new feeder [23]

3. Results and discussion

3.1. Structural properties

Fig.2 gives a comparison among the XRD patterns of 100, 300 and 500 nm thick ZnS films. All samples have cubic structure (a=b=c=5.406 Å) with a [111] preferred orientation at 2θ = 28.93º which showed improvement upon film thickness increment. Similar pattern of XRD for ZnS thin films made by thermal evaporation was reported in literature [14].

Increasing film thickness from 100nm to 500nm not only intensified the characteristics peak of ZnS, but also led to appearance of two other peaks in the XRD pattern due to improvement of its crystallinity. This matter may be attributed to the temperature increment of the substrate due to higher thickness and deposition time as stated by Wu et al [14].

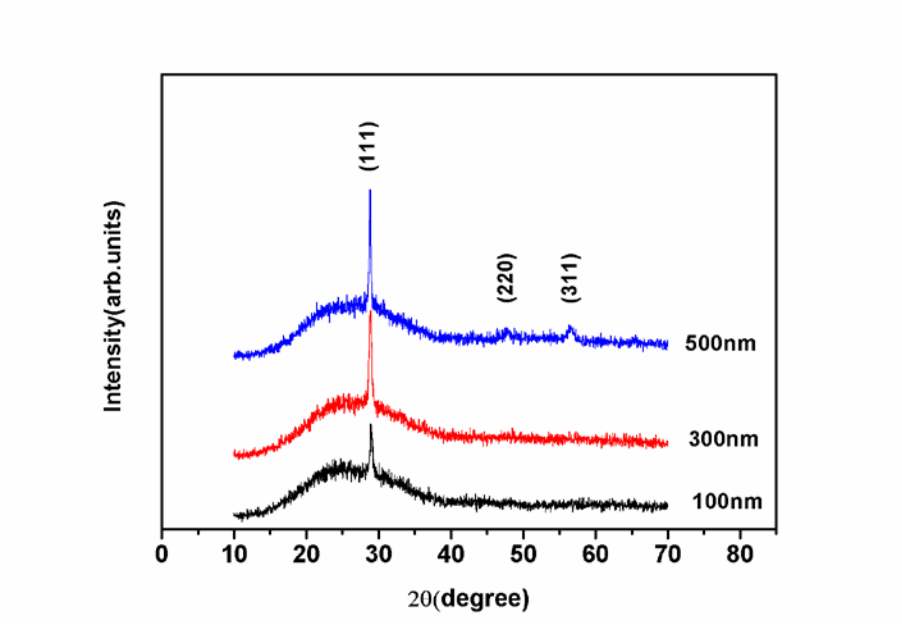

Fig.2: XRD pattern of 100,300 and 500 nm ZnS thin films

3-2 Optical properties

Optical studies were performed by measuring the absorbance and transmittance of ZnS films of 100nm, 300nm and 500nm on glass substrates in the wavelength region of 250–1100 nm. The absorbance spectra of samples are shown in Fig.3. It is observed from the figure that, the optical absorptions in the visible region is smaller than those in the ultraviolet region. It is also seen that the absorption value in the ultraviolet region increased slightly with increasing the sample thickness.

Fig.4 shows the transmittance spectra of the ZnS films with different thicknesses obtained at room temperature. In all samples, the transmittance decreases abruptly in the short wavelengths, corresponding to below band gap region which is due to the band edge absorption. It is clearly seen that the optical transmission is more than 90% for ZnS thin film with 100nm thick which decreases to 70% upon increasing the thickness to 500nm. It is worth noting that the number of fringes increases by increasing the film thickness which is a common observation.

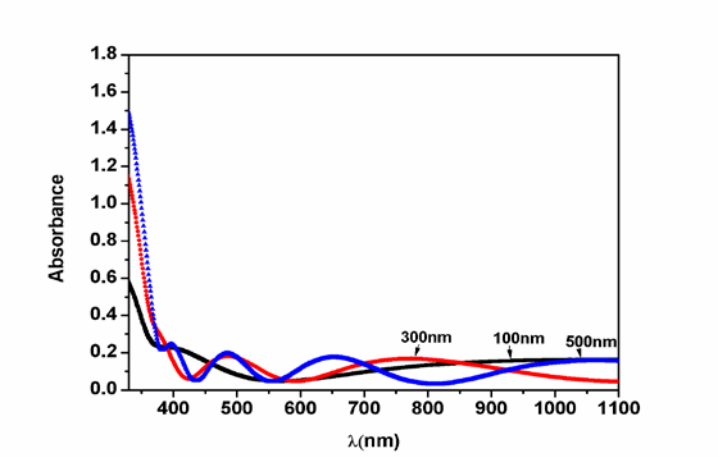

Fig.3: Absorbance spectra of 100, 300 and 500 nm ZnS thin films

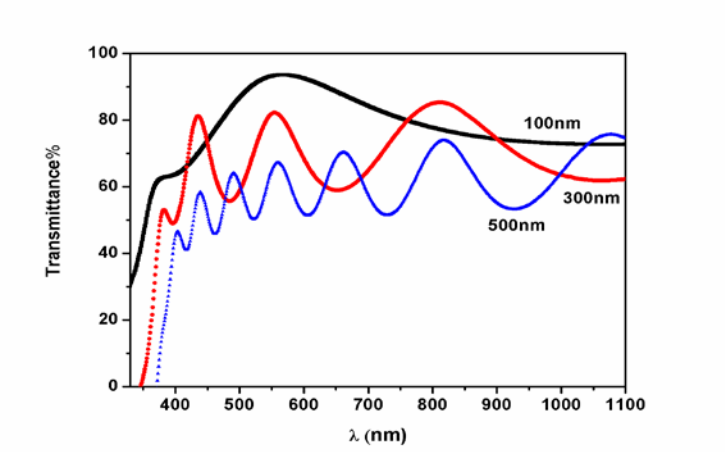

Fig.4: Transmitnce spectra of 100,300 and 500 nm ZnS thin films

The absorption coefficient (α) was analyzed using the following expression for near-edge optical absorption of semiconductors [24]:

$$\alpha h\nu = K\,(h\nu - E_g)^{1/2} \qquad (1)$$

Where K is a constant and E_g is the separation between the valance and conduction bands. The band gap values were determined from the intercept of the straight-line portion of the $(\alpha h\nu)^2$ against the hν graph on the hν-axis using computer fitting program. The linear part shows that the mode of transition in these films is of direct nature.

Fig.5 gives the plot of $(\alpha h\nu)^2$ in terms of band gap for ZnS films. As specified in the figure, band gap of the deposited ZnS films of 100nm, 300nm and 500nm thick are 3.25 eV, 3.35 eV and 3.45 eV respectively. The band gap of 500nm sample is closer to bulk cubic phase (~3.5eV) and single crystal ZnS (~3.6 eV) values than that of other samples.

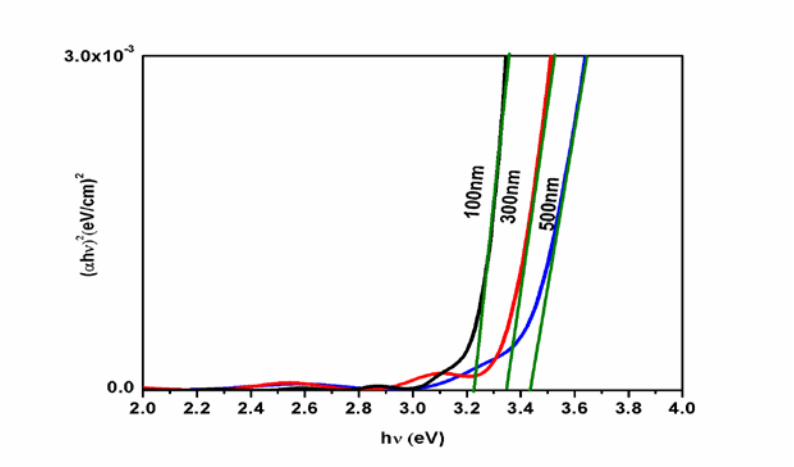

Fig.5: Plot of $(\alpha h\nu)^2$ Vs. $h\nu$ for 100nm, 300nm and 500 nm ZnS thin films

It can be attributed to the improvement in the films crystallinity as supported by the XRD studies. In the case of films with 100nm and 300nm thick, the bang gaps are lesser than the bulk value which can be attributed to the creation of allowed energy states in the band gap at the time of film preparation [28]. Similar effect has been observed for CBD grown ZnS films [29] and CdS films [30].

The average refractive index (n) of samples was retrieved from all the normal incidence transmittance data by observing the position of the maxima and minima with respect to the wavelengths (λ) of the incident beam (visible region) which was suggested by Swanepoel [25] and the results are presented in Figs.6-8. The calculated values of refractive indices of the different films are comparable with the reported values [14, 26, and 27]. It is observed in the three figures that the refractive index in all the samples have similar behavior in all the spectral region, that is, it increases gradually as the light wavelength increases. The values of refractive index at any wavelength were found higher in the case of thicker film. It can be seen that, for all the specimens, as the wavelength is increased, the refractive index decreases gradually and reaches to a certain value.

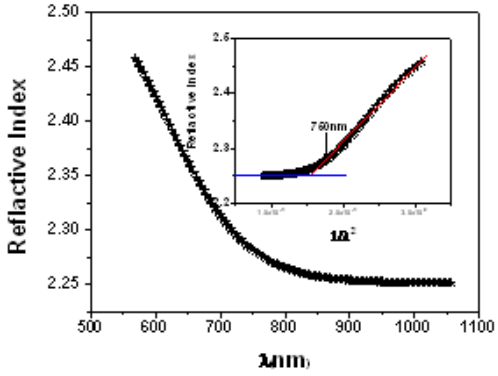

Fig.6: Refractive index for 100nm

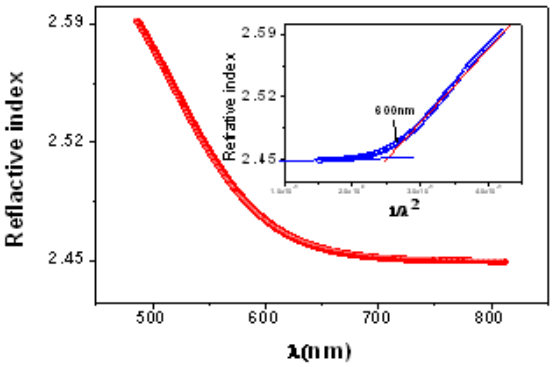

Fig.7: Refractive index for 300nm

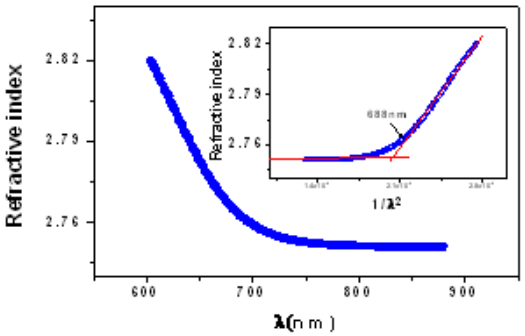

Fi.g8: Refractive index for 500nm

Considering the XRD and band gap results, the reduction in the refractive indices of the deposited ZnS samples with thickness may be attributed to the creation of voids (sulfur vacancy) on the sample surface. This phenomenon was also observed and interpreted as being due to the increase of the volume fraction of the voids available on the film surface or to the increase of the carrier concentration as reported in the case of sol-gel deposited ZnO thin film [31].

In addition, the refractive index versus $1/\lambda^2$ has been drown for the three samples and shown at top right corner of each figures of 6 to 8 correspondingly. The drown curves follow the Coushi equation ($n=a+b/\lambda^2$) behavior below 700nm wavelength for all the samples.

4. Conclusion

Flash evaporation technique equipped by a new designed feeder was employed to deposit ZnS thin films with different thicknesses. The structural and optical properties of the prepared samples were studied. All the samples showed cubic structure with a [111] preferred orientation. The increase in film thickness was found to improve the film crystallinity. From transmittance spectra of the samples it was found that the increase in film thickness led to the fall in the transmittance. The film thickness increment enhanced the band gap energy to a value near to that of the ZnS single crystal. The refractive index of the samples was found to increase with film thickness.

References

[1] M. P. Valkonen, S. Lindroos, M. Leskela, Appl. Surf. Sci. **134**, 283 (1998).
[2] K. R. Murali, A.C. Dhanemozhi, R. John, J. Alloys & Comp. **464**, 383 (2008).
[3] Y. Yang, W. Zhang, Mater. Lett. **58**, 3836 (2004).
[4] P. Roy, J. R. Ota, S. K. Srivastava, Thin Solid Films **515**,1912 (2006).
[5] Y. Ni, G. Yin, J. Hong, Z. Xu, Mater. Res. Bull. **39**, 1967 (2004).
[6] T. Kryshtab, V. S. Khomchenko, J. A. Andraca-Adame, V. E. Rodionov, V. B. Khachatryan, Yu. A. Tzyrkunov, Superlattices and Microstructures **40**, 651 (2006).
[7] M. A. Tagliente, M. Penza, M. Gusso, A. Quirini, Thin Solid Films **353**, 129 (1999).
[8] P. K. Ghosh, S. Jana, S. Nandy, K. K. Chattopadhyay, Mater. Res. Bull. **42**, 505 (2007).
[9] W. Daranfed, M. S. Aida, A. Hafdallah, H. Lekiket, Thin Solid Films **518 ,** 1082 (2009).
[10] T. Ben Nasr, N. Kamoun, C. Guasch, Appl. Surf. Sci. **254**, 5039 (2008).
[11] M. Gunasekaran, R. Gopalakrishnan, P. Ramasamy, Mater. Lett. **58**, 67 (2003).
[12] F. Loglio, M. Innocenti, G. Pezzatini, M. L. Foresti, J. Electroanalytical Chem. **562**, 117 (2004).
[13] S.Yano, R. Schroeder, B. Ullrich, H. Sakai, Thin Solid Films **423**,273 (2003).
[14] X. Wu, F. Lai, L. Lin, J. Lv, B. Zhuang, Q. Yan. Z. Huang, Appl. Surf. Sci. **254**, 6455 (2008).
[15] T. G. Kryshtab, V.S. Khomchenko, V. P. Papusha, M. O. Mazin, Yu. A. Tzyrkunov, Thin Solid Films **403 – 404**, 76 (2002).
[16] X. K. Duan, Y. Z. Jiang, Thin Solid Films **519**, 3007 (2011).
[17] M. M. El-Nahass, A. A. M. Farag, H. S. Soliman, Optics Communications, **284**, 2515 (2011).
[18] X. K. Duan, Y. Z. Jiang, Appl. Surf. Sci. **256**, 7365 (2010).
[19] R. N. Gayen, S. N. Das, S. Dalui, R. Paul, R. Bhar, A. K. Pal, Thin Solid Films, **518,** 3595 (2010).
[20] B. H. Patel, S. S. Patel, Cryst. Res. Technol. **41**, 117 (2006).
[21] N. M. Shah, J. R. Ray, V. A. Kheraj, M. S. Desai, C. J. Panchai, J. Matter. Sci. **44**, 316 (2009).
[22] K. R. Murali, C. Kannan, K. Subramanian, Chalcog. Lett. **5**, 195 (2008).
[23] M. H. Ehsani, H. Rezagholipour dizaji,Chalcog.Lett. **8**, 33 (2011).
[24] R. Ghaffar Motedayen Aval, A. Goudarzi, J. Alloys & Comp. **466**, 488 (2008).
[25] R. Swanepoel, J. Phys. E , Sci.Instrum. **16,** 1214 (1983).
[26] F.Gode, Physica B, (2010) IN PRESS.
[27] S. Ilican, Y. Caglara, M. Caglara, F. Yakuphanoglub, J. Alloys & Comp. **480**, 234 (2009).
[28] P.P.Sahay,R. K.Nath,S.Tewari,Crys.Res.Technol.**42**,275 (2007).
[29] S. A. Vanalakar, S. S. Mali, M. P. Suryavanshi, P. S. Patil.Digest .Journal of Nanomaterials and Biostructures **5,**805 **(**2010).
[30] S. D. Sartale, B. R. Sankapal, M. Lux-Steiner, A. Ennaoui, Thin Solid Films **480–481** 168 (2005).
[31] J. Lv, K.Huang, X. Chen, J. Zhu, C. Cao, X. Song, Z. Sun, Optics Communications (2011) IN PRESS